Tri Dasa Mega Vol. 22 No. 1 (2020) 17–22

Jurnal Teknologi Reaktor Nuklir

Tri Dasa Mega

Journal homepage: jurnal.batan.go.id/index.php/tridam

The Radioactivity Estimation of The Irradiated 13 MeV Cyclotron's Concrete Shield

Isdandy Rezki Febrianto*, Puradwi Ismu Wahyono, Suharni

Center for Accelerator Science and Technology (PSTA) – National Nuclear Energy Agency (BATAN), Jl. Babarsari, Yogyakarta, 55281, Indonesia

ARTICLE INFO

Article history:

Received: 25 February 2020
Received in revised form: 17 March 2020
Accepted: 18 March 2020

Keywords:

Radioactivity
Concrete Shield
13 MeV Cyclotron
Neutron Irradiation
DECY-13
PHITS

A B S T R A C T

The Center for Accelerator Science and Technology (PSTA) planned to install K500 concrete shield in its 13 MeV cyclotron facility (DECY-13). However, fast neutrons that are generated by this cyclotron could activate materials of the concrete. It may harm the radiation workers. In this work, we conducted simulations using ORIGEN2 and PHITS computer code to estimate the formed radioactivity and the neutron flux distribution in the DECY-13 cyclotron's concrete shield. Based on the simulation, the induced radioactivity is 2.3478 × 10^9 Bq, while its gamma dose rate is 22.09 μSv/m^2h. The most contributed isotopes are Th-233, Ho-166, Al-28, Mn-56 and Si-31. This dose is quite high. Neutron fluxes in the rear of the simulated concrete shield are also still prominent. Accordingly, it is necessary to attach neutron shielding materials which do not generate high-intensity gamma-ray. The formed radioactivity is high; but it appears from the short half-life isotopes such as Th-233, Ho-166, Al-28, Mn-56 and Si-31. Its activity will diminish quickly after the cyclotron is off. Hence, it will be safe for radiation workers.

1. INTRODUCTION

In recent years, the Centre for Accelerator Science and Technology (PSTA) has developed 13 MeV cyclotron (DECY-13) for the fluorine-18 production [1–5]. This cyclotron generates secondary gamma and neutron, referring to the previous analysis [6]. Therefore, the radiation shield with K500 concrete quality will be installed to reduce gamma exposure. It is the same material as previously used on its target module, for the experiment of proton beam energy measurements. In other hands, neutron might activate materials, including concrete. Radiation caused by the activated concrete material can endanger the radiation workers.

The other researchers have examined the activation of concrete in the nuclear reactors [7] and accelerators [8]. However, materials of concrete may differ depending on their sand, cement, and aggregate. In this case, the sand applied for concrete shields on the DECY-13 is Progo sand. The study elsewhere mentions that Progo sand contains thorium and the rare earth metal [9]. These elements are uncommon in the concrete. Furthermore, the previous analysis informs that DECY-13 produces mostly fast neutron [6]. It is distinct from preceding examinations using thermal neutrons [10]. Hence, the objective of this paper is to find out the formed radioactivity and the neutron flux distribution in the DECY-13's concrete shield.

The investigations elsewhere employed the ORIGEN2 [11, 12] and PHITS [13, 14] computer code in the various nuclear field. Both software is known to be reliable [15–17]. Accordingly, we used ORIGEN2 and PHITS to estimate the radioactivity

*E-mail: isdandy.rezki@batan.go.id
DOI: 10.17146/tdm.2020.22.1.5801

in the irradiated 13 MeV cyclotron's concrete shield.

2. METHODOLOGY

DECY-13 implements the concrete shield with a density of 2.3 g/cm3. We conducted the Energy Dispersive X-Ray Fluorescence (EDXRF) analysis to acquired its elemental data.

ORIGEN2 performs calculations based on 1 gram of the concrete sample, for the simplicity in obtaining the specific activity. It is a commonly used unit in the radiation protection field. It describes the radioactivity concentration (Bq/g) of radionuclide in the material.

In ORIGEN2 calculation, we assumed the concrete sample as a slab with 1 cm length, since it has a density of 2.3 g/cm^3, then its cross-section is 0.434783 cm^2. These calculations utilized a neutron source of 1.91 × 10^{11} neutrons/s, referring to the previous analysis [6]. Duration of irradiation was 1 hour. The radioactivity value procured from this algorithm is conservative because it ignores its distribution. PHITS also take an identical concrete sample for the simulation with monodirectional 1.5 MeV neutron source. Additionally, we varied the neutron energy and the duration of irradiation to find out its effect on the formed radioactivity.

PHITS applies the isotropic neutron source to examine radioactivity distribution. In these simulations, PHITS models the concrete as a large block with dimensions of 120 cm x 120 cm x 120 cm. There are small cubes with a size of 15 cm x 15 cm x 15 cm that arranged inside the block, regarding their axial (x) and radial (y) position as in Fig. 1. It is intended to estimate the neutron flux and radioactivity on the specific region. PHITS execute the [T-Track] and [T-DCHAIN] tally to obtain such value [18].

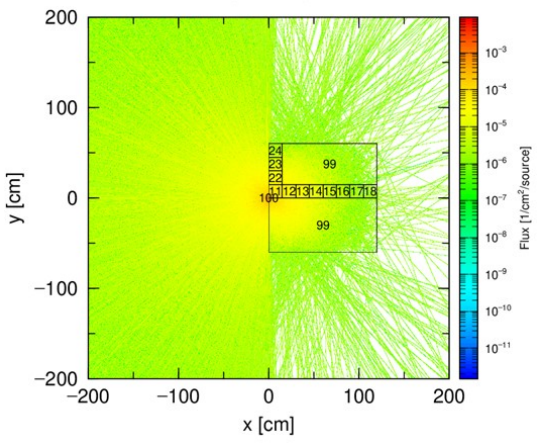

Fig. 1. Model of the concrete that irradiated by the isotropic neutron source

3. RESULTS AND DISCUSSION

The Energy Dispersive X-Ray Fluorescence (EDXRF) results confirm that the DECY-13's concrete shield contains thorium in the form of ThO_2 and the rare earth metal oxides such as CeO_2, Er_2O_3, Eu_2O_3, Gd_2O_3, Ho_2O_3, Pm_2O_3, Tb_4O_7 and Y_2O_3. Table 1 shows its elemental content. ORIGEN2 uses all of these data, while PHITS dismiss the erbium (Er) and promethium (Pm). PHITS also replaces the natural lead with Pb-208 isotope.

Table 1. EDXRF result of DECY-13's concrete shield

Oxide	Concentration (%)	Oxide	Concentration (%)
MgO	0.409	SrO	0.202
Al2O3	9.954	Y2O3	0.008
SiO2	36.308	ZrO2	0.029
SO3	0.939	Nb2O5	0.001
Cl	0.010	SnO2	0.034
K2O	1.484	TeO2	0.015
CaO	38.518	BaO	0.048
TiO2	1.181	CeO2	0.016
V2O5	0.042	Pm2O3	0.025
MnO	0.164	Eu2O3	0.033
Fe2O3	10.289	Gd2O3	0.031
CuO	0.011	Tb4O7	0.129
ZnO	0.023	Ho2O3	0.005
Ga2O3	0.004	Er2O3	0.025
As2O3	0.002	PbO	0.002
Rb2O	0.006	ThO2	0.053

Figure 2 illustrates 1 gram of concrete sample that irradiated by the monodirectional neutron source. Referring to ORIGEN-2 calculation, the activation products such as europium (Eu), aluminium (Al), manganese (Mn), vanadium (V) and silicon (Si) dominate the formed radioactivity. The specific activity of the irradiated concrete is 9.66 × 10^7 Bq/g. It is different from PHITS that resulted in 4.35 × 10^6 Bq/g. The considerable radioactivity comes from aluminium (Al), thorium (Th), barium (Ba), silicon (Si) and manganese (Mn). The distinction on the neutron source energy and the concrete composition applied by ORIGEN-2 and PHITS, cause the outcome to be unidentical. ORIGEN2 implements

thermal neutron source, whereas PHITS utilizes 1.5 MeV monoenergetic neutron source.

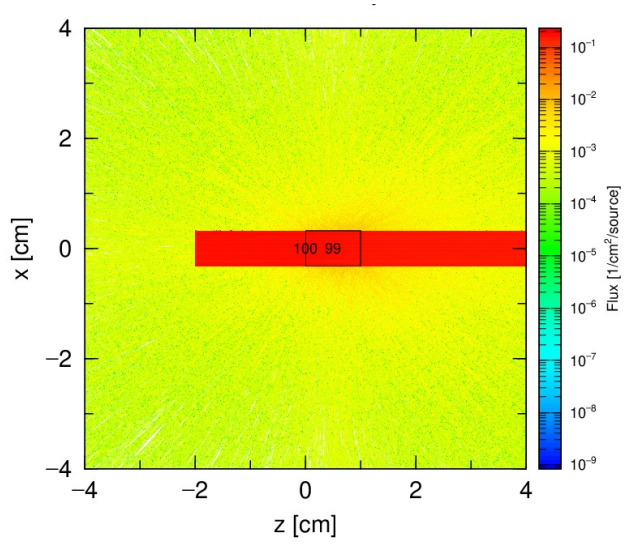

Fig. 2. Neutron flux on the concrete that irradiated by the monodirectional neutron source

In the fast neutron spectrum, the specific radioactivity of the irradiated concrete with an hour of irradiation based on PHITS simulation is lower than ORIGEN2 calculation. ORIGEN2 uses a conservative approach, in contrast to PHITS which is more realistic. Based on PHITS, specific radioactivity significantly increases, along with the decrease in neutron source energy, as in Fig. 3. Its trend is related to the probability of neutron interaction that is larger in the low energy spectrum, compared to the higher energy. At the source energy of 10 eV, it becomes equal to the ORIGEN2 result. It is in consequence of the thermal neutrons used by default in the ORIGEN2 calculation.

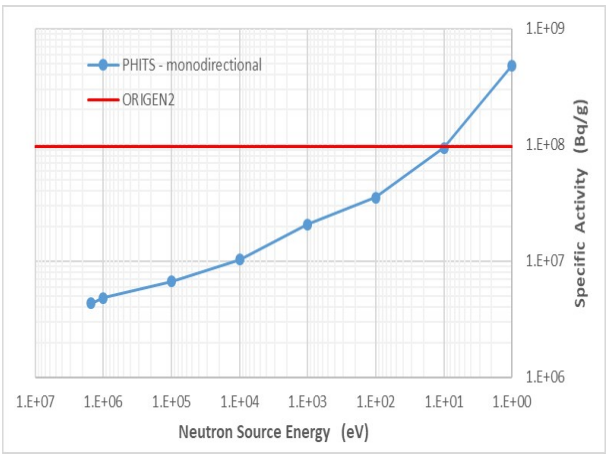

Fig. 3. The effect of neutron source energy to the specific radioactivity of the concrete shield

Based on the PHITS simulation, the irradiation duration raises the specific radioactivity of the concrete shield, as displayed in Fig. 4. Its trend is logarithmic. This trend is related to the neutron fluence buildup and the decay of formed radioactive materials. The irradiation duration increases the neutron fluence and the probability of neutron interaction. Hence, the radioactivity rises. But, the formed radioisotopes are decaying along with time. Therefore, it compensates the increasing caused by neutron fluence and makes the trend logarithmic. Nonetheless, it does not remarkably rise, compared to the effect of neutron energy.

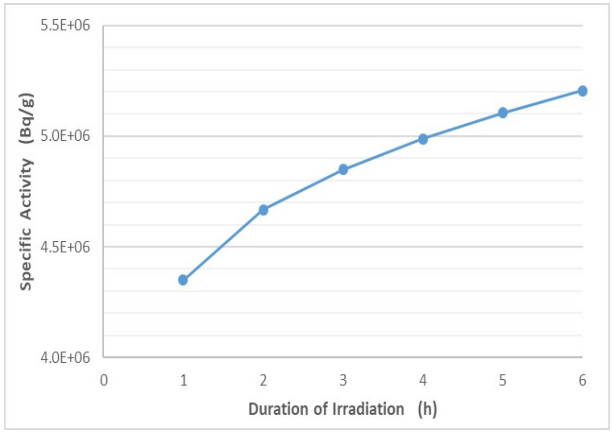

Fig. 4. The influence of irradiation duration to the specific radioactivity of the concrete shield

The ORIGEN2 and PHITS calculation on the sample, cannot describe the condition of the entire concrete shield, because the flux and energy of the neutron are not constant along its journey. The concrete might moderate or even absorb the neutron beam. It is necessary to find out the distribution of the neutron flux and the formed radioactivity on the entire concrete shield. The solution is PHITS employ the full concrete block at a distance of 2 cm from the isotropic neutron source. Inside it, there are small cubes arranged on the x (axial) and y (radial) axis, as in Fig. 1. The coloured line represents neutron flux per source current. There are gradations of colour that show the flux differences in each region.

Total radioactivity that formed due to an hour of irradiation, in the whole concrete shield, is 2.3478 × 10^9 Bq. The prominent radioisotopes are Th-233, Ho-166, Al-28, Mn-56 and Si-31. Since Al-28 and Mn-56 emit high energetic gamma, thus both dominate the gamma dose rate of the irradiated concrete. The values are 11.25 and 9.26 μSv/m^2h respectively from a total of 22.09 μSv/m^2h. This gamma dose is quite high for the radiation workers. Figure 5 provides a detailed radioisotopes chart.

Ho-166 and Mn-56 have a relatively long half-live compared to Th-233. After 2 hours of irradiation, both dominate the formed radioactivity, replacing Th-233. Mn-56 also supersede Al-28 in the gamma dose rate with 16.34 μSv/m^{2}h. It is because the formation rate of the short half-life radioisotopes cannot compensate for its decay rate compared to the relatively long half-life ones.

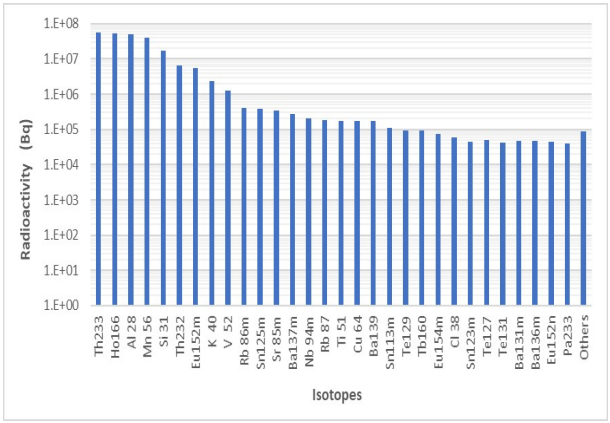

Fig. 5. Radioisotopes chart of the irradiated concrete

Figure 6 explains the neutron flux distribution in the concrete shield. The flux decreases along with increasing distance, both on axial and radial. However, neutron flux in the axial position is generally higher than radial ones. It was caused by neutron source distance to the concrete, which is further in the radial position. Neutron fluxes in the rear of the simulated concrete shield are substantial, ranging in order of 10^5 to 10^6 neutrons/cm^{2}s. Therefore, it is needed to apply neutron shielding materials.

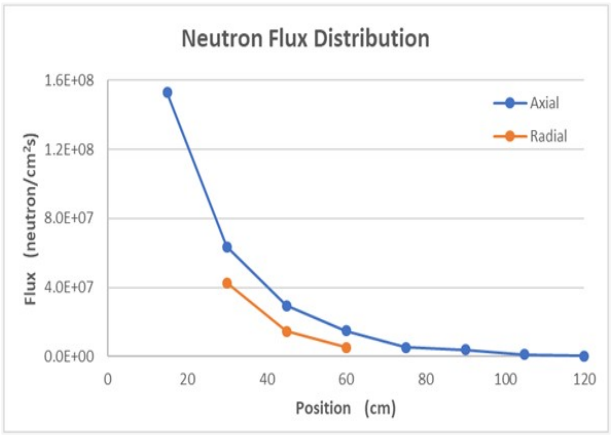

Fig. 6. Neutron flux distribution on the irradiated concrete shield

The induced radioactivity increases from the axial position of 15 to 45 cm. Afterwards, it starts to attenuate, as shown in Fig. 7. But in the radial ones, it decreases from the beginning. The peak of radioactivity in the axial may be related to the nuclear cross-section, which is influenced by the incoming neutron energy. The cross-section represents the probability of interactions that might occur. The probability of neutron interaction is greater in the low energy neutron, compared to the fast one.

Neutrons are decelerating and lost its energy while passing through the concrete. If the neutron energy is decreasing, then its cross-section and the probability of absorption interaction are increasing. As a result, concrete materials absorb more neutrons. Hence, its radioactivity increases. This trend continues until neutron flux is not sufficient, thus, the radioactivity decrease. Based on the calculation using ORIGEN2 and PHITS, the formed radioactivity in the DECY-13's concrete shield caused by the fast neutron irradiation is quite high. These radionuclides also generate high gamma dose. The neutron absorber materials with low gamma emission are required. Thus, the gamma dose received by the radiation workers does not exceed the threshold.

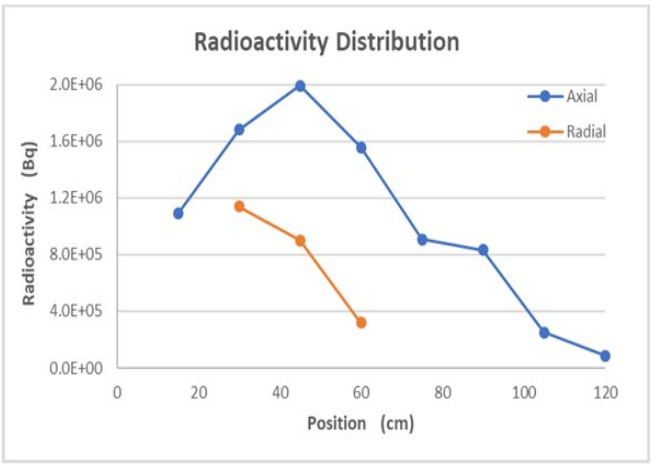

Fig. 7. Radioactivity distribution in the irradiated concrete shield

4. CONCLUSION

The specific activity of DECY-13's concrete shield, based on a conservative approach with ORIGEN2 and PHITS is 9.66 × 10^7 Bq/g and 4.35 × 10^6 Bq/s respectively. Based on PHITS simulation, total radioactivity in the entire concrete shield is 2.3478 × 10^9 Bq, while its gamma dose rate is 22.09 μSv/m^{2}h. It is quite high for radiation workers. Neutron fluxes in the end side of the simulated concrete shield are also noticeable. Accordingly, neutron absorber materials which do not produce high-intensity gamma-ray is needed. Although the formed activity and gamma dose rate is quite high, it

comes from the relatively short half-life isotopes such as Th-233, Ho-166, Al-28, Mn-56 and Si-31. Hence, its activity will decrease along with non-operational time.

ACKNOWLEDGMENT

The authors would like to thank the director and all staff of the Center for Accelerator Science and Technology (PSTA) – National Nuclear Energy Agency (BATAN) for their support.

REFERENCES

[1]. Iswining F., Suprapto, Taufik, Kurnia W., Dyah Optimation of DECY-13 cyclotron magnet mapping system (Optimasi sistem pemetaan magnet siklotron DECY-13). GANENDRA Majalah IPTEK Nuklir. 2016. **19**(2):55–63.

[2]. Silakhudin Determining the results of radioisotope product in DECY-13 cyclotron facility (Penentuan hasil produk radioisotop fluor-18 pada fasilitas siklotron DECY-13). Jurnal Penelitian Saintek. 2016. **21**(1):1–9.

[3]. Silakhuddin I.A.K. Optimization of ion source head position in the central region of DECY-13 cyclotron. Atom Indonesia. 2017. **43**(2):81–6.

[4]. F. S. Permana, I. A. Kudus, Taufik K.W. Comparation of construction and simulation result from isochronus of cyclotron magnet DECY-13 (Perbandingan hasil konstruksi terhadap hasil simulasi dari isokronus magnet siklotron DECY-13). GANENDRA Majalah IPTEK Nuklir. 2017. **20**(2):83.

[5]. Saefurrochman Analysis of the PD plus gravity control as a position controller device of DECY-13 ion source (Analisis kendali PD plus gravity untuk perangkat pengatur posisi sumber ion DECY-13). Jurnal Forum Nuklir. 2018. **12**(1):17–28.

[6]. Tursinah, Rasito; Bunawas; Taufik; Sunardi; Suryanto H. Designing of radiation shield for the DECY-13 cyclotron using monte carlo method (Desain perisai radiasi untuk siklotron DECY-13 menggunakan metode monte carlo). in: *Prosiding Pertemuan dan Presentasi Ilmiah - Penelitian Dasar Ilmu Pengetahuan dan Teknologi Nuklir 2016*. Surakarta. 2016. pp. 231–5.

[7]. Hajdú D., Dian E., Klinkby E., Cooper-Jensen C.P., Osán J., Zagyvai P. Neutron activation properties of PE-B4C-concrete assessed by measurements and simulations. Journal of Neutron Research. 2019. **21**:87–94.

[8]. Kumagai M., Sodeyama K., Sakamoto Y., Toyoda A., Matsumura H., Ebara T., et al. Activation reduction method for a concrete wall in a cyclotron vault. Journal of Radiation Protection and Research. 2017. **42**(3):141–5.

[9]. Irzon R. Geochemical character of coastal sediments from southern kulon progo with implications for provenance (Komposisi kimia pasir pantai di selatan kulon progo dan implikasi terhadap provenance). Jurnal Geologi dan Sumberdaya Mineral. 2018. **19**(1):31–46.

[10]. Okuno K., Tanaka S. Activation experiment for concrete blocks using thermal neutrons. EPJ Web of Conferences. 2017. **153**:2–6.

[11]. Noh T. yang, Park B.G., Kim M.S. Estimation of nuclear heating by delayed gamma rays from radioactive structural materials of HANARO. Nuclear Engineering and Technology. 2018. **50**(3):446–52.

[12]. Ain Sulaiman S.N., Mohamed F., Rahim A.N.A.B., Kassim M.S., Hamzah N.S. Source term atmospheric release and core inventory analysis for the puspati triga reactor under severe accident conditions. Sains Malaysiana. 2019. **48**(10):2277–84.

[13]. Wang H., Otsu H., Sakurai H., Ahn D.S., Aikawa M., Doornenbal P., et al. Spallation reaction study for fission products in nuclear waste: Cross section measurements for 137Cs and 90Sr on proton and deuteron. Physics Letters, Section B: Nuclear, Elementary Particle and High-Energy Physics. 2016. **754**:104–8.

[14]. Wang H., Otsu H., Sakurai H., Ahn D., Aikawa M., Ando T., et al. Spallation reaction study for the long-lived fission product 107Pd. Progress of Theoretical and Experimental Physics. 2017. **2017**(2):1–10.

[15]. Yamamoto T., Iwahashi D. Validation of decay heat calculation results of ORIGEN2.2 and CASMO5 for light water reactor fuel. Journal of Nuclear Science and Technology. 2016. **53**(12):2108–18.

[16]. Iwamoto Y., Sato T., Hashimoto S., Ogawa T., Furuta T., Abe S.I., et al. Benchmark study of the recent version of the PHITS code. Journal of Nuclear Science and Technology. 2017. **54**(5):617–35.

[17]. Takada K., Sato T., Kumada H., Koketsu J.,

Takei H., Sakurai H., et al. Validation of the physical and RBE-weighted dose estimator based on PHITS coupled with a microdosimetric kinetic model for proton therapy. Journal of Radiation Research. 2018. **59**(1):91–9.

[18]. Sato T., Iwamoto Y., Hashimoto S., Ogawa T., Furuta T., Abe S. ichiro, et al. Features of particle and heavy ion transport code system (PHITS) version 3.02. Journal of Nuclear Science and Technology. 2018. **55**(6):684–90.